The EMBO Journal Vol. 22 No. 21 pp. 5666–5678, 2003

Nogo-A at CNS paranodes is a ligand of Caspr: possible regulation of K^+ channel localization

Du-Yu Nie[1,2], Zhi-Hong Zhou[1], Beng-Ti Ang[1,2,3], Felicia Y.H.Teng[4], Gang Xu[1], Tao Xiang[1,3,5], Chao-yang Wang[1,2], Li Zeng[6], Yasuo Takeda[7], Tian-Le Xu[8], Yee-Kong Ng[2], Catherine Faivre-Sarrailh[9], Brian Popko[10], Eng-Ang Ling[2], Melitta Schachner[11], Kazutada Watanabe[7,12], Catherine J.Pallen[6,13,14], Bor Luen Tang[4,14] and Zhi-Cheng Xiao[1,2,14]

[1]Department of Clinical Research, Singapore General Hospital, [2]Department of Anatomy, National University of Singapore, [3]National Neuroscience Institute, [4]Department of Biochemistry and Neurobiology Program, Office of Life Sciences, National University of Singapore, [6]Institute of Molecular and Cell Biology, Singapore, [5]Department of Anatomy, Sichuan University, Chengdu, [8]School of Life Science, University of Science and Technology of China, Hefei, China, [7]Department of Cell Recognition, Tokyo Metropolitan Institute of Gerontology, Tokyo, [12]Department of Bioengineering, Nagaoka University of Technology, Nagaoka, Japan, [9]Neurobiologie de Interactions Cellulaires et Neuropathologie, FRE 2533, Institut Jean Roche, Marseilles, France, [10]The Jack Miller Center for Peripheral Neuropathy, University of Chicago, Chicago, IL, USA, [11]Zentrum fur Molekulare Neurobiologie, University of Hamburg, Hamburg, Germany and [13]Department of Pediatrics, University of British Columbia, BC Research Institute for Children's and Women's Health, Vancouver, BC, Canada

[14]Corresponding authors
e-mail: gcrxzc@sgh.com.sg, mcbtbl@imcb.nus.edu.sg or cpallen@interchange.ubc.ca

We report Nogo-A as an oligodendroglial component congregating and interacting with the Caspr–F3 complex at paranodes. However, its receptor Nogo-66 receptor (NgR) does not segregate to specific axonal domains. CHO cells cotransfected with Caspr and F3, but not with F3 alone, bound specifically to substrates coated with Nogo-66 peptide and GST–Nogo-66. Binding persisted even after phosphatidylinositol-specific phospholipase C (PI-PLC) removal of GPI-linked F3 from the cell surface, suggesting a direct interaction between Nogo-66 and Caspr. Both Nogo-A and Caspr co-immunoprecipitated with Kv1.1 and Kv1.2, and the developmental expression pattern of both paralleled compared with Kv1.1, implicating a transient interaction between Nogo-A–Caspr and K^+ channels at early stages of myelination. In pathological models that display paranodal junctional defects (EAE rats, and *Shiverer* and $CGT^{-/-}$ mice), distances between the paired labeling of K^+ channels were shortened significantly and their localization shifted toward paranodes, while paranodal Nogo-A congregation was markedly reduced. Our results demonstrate that Nogo-A interacts *in trans* with axonal Caspr at CNS paranodes, an interaction that may have a role in modulating axon–glial junction architecture and possibly K^+-channel localization during development.

Keywords: Caspr/K^+ channel/Nogo-A/Nogo-66 receptor/paranode

Introduction

During myelination, there is a complex, yet precise and efficient, process that ensures the congregation of specific ion channels and other related molecules to distinct segments along the axon. Establishment and maintenance of the molecular architecture of axonal domains are critical to ensure rapid saltatory conduction of nerve impulses. The nodes of Ranvier are enriched in Na^+ channels whilst K^+ channels are excluded from this location and instead occupy juxtaparanodal regions. However, during the early stages of both developmental myelination and remyelination, K^+-channel congregates are transiently located at the paranodal region (Rasband *et al*., 1998; Vabnick *et al*., 1999) between the nodes and juxtaparanodes. This is where the glial cytoplasmic loops come into contact with the axolemma. Three adhesion molecules, Caspr, F3/contactin and neurofascin 155, exist in a *trans*-triple complex, and constitute an essential scaffold for the maintenance of the architecture of the axoglial apparatus at the paranodes (Girault and Peles, 2002). Caspr is a transmembrane protein with an extracellular domain that contains a series of laminin-G-like domains and EGF repeats (Peles *et al*., 1997). F3 is required for the coordinated transport of Caspr and Na^+ channels to the cell surface (Faivre-Sarrailh *et al*., 2000; Kazarinova-Noyes *et al*., 2001). Studies on dysmyelinating mouse mutants deficient in myelin-related and axonal proteins, such as ceramide galactosyl transferase (CGT) (Popko, 2000; Ishibashi *et al*., 2002), F3/contactin (Boyle *et al*., 2001) and Caspr (Bhat *et al*., 2001), as well as myelin basic protein (*Shiverer* mice) (Rasband and Trimmer, 2001), have shown that clustering of axonal domain constituents and the exact localization of ion channels, particularly K^+ channels, are dependent on communication between axons and oligodendroglia. However, the molecular mechanisms that regulate the accumulation of K^+ channels into discrete zones are not entirely clear.

Nogo-A has been extensively studied in the context of CNS regeneration and is one of the pivotal factors in the inhibition of axonal regeneration after injury (Woolf, 2003). All three isoforms of Nogo (A, B and C) share the same C-terminus with two transmembrane domains and an extracellular 66 amino acid loop (Nogo-66). Nogo-A has a large cytoplasmic N-terminal domain (Nogo-N) not found in Nogo-B or Nogo-C. Regeneration phenotypes

in Nogo-A-deficient mice were not particularly unequivocal, and the exact role of Nogo-A in the CNS remains to be investigated (Woolf, 2003).

Knowledge of Nogo-A and NgR distribution at the interface between neurons and oligodendrocytes will be important in understanding their roles in CNS development. In the present study, we demonstrate that Nogo-A is found to localize to paranodes, where it interacts with the paranodal junction protein Caspr. This interaction may play a role in regulating the location of K^+ channels along the axon during the early stages of myelination.

Results

Nogo-A is localized to the paranodes of myelinated axons

The distribution of Nogo-A was examined along the white matter tracts of adult rat brainstem. In longitudinal sections, similar localization patterns of Nogo-A were observed with two different Nogo-A antibodies developed in our laboratory (Figure 1A, a–f) (Liu *et al*., 2002) and that of Dr Stephen Strittmatter (Figure 1A, g–i) (Wang *et al*., 2002). By double immunofluorescence labeling with Kv1.1 (red) (Figure 1A, a–c, g–i) or the Na^+ channel (red) (Figure 1A, d–f), Nogo-A immunoreactivity (green) was confined specifically to paranodal segments along myelinated axons (Figure 1A), which flank nodal Na^+ channel labeling and juxtaparanodal Kv1.1 labeling, thus reflecting its paranodal location. Similar observations were made in other nerve-fiber-rich CNS sites such as the corpus callosum and the spinal cord (not shown). The specific labeling of Nogo-A in axonal domains was undetectable after the Nogo-A antisera (1:200) were preincubated with 100-fold molar excess of antigen (Figure 1A, j). These observations suggest that Nogo-A may be enriched at the paranode and is a component of the paranodal protein complex.

The specific paranodal location of Nogo-A was further investigated using immunoelectromicroscopy (IEM). Consistent with previous observations (Huber *et al*., 2002), Nogo-A immuno-reactivity was high in the inner and outer loops of the myelin sheath (Figure 1B, a) and low in compact myelin of rat spinal cord (Figure 1B, b). Notably, in longitudinal sections, Nogo-A immunoreactivity was high in the expanded terminal glial loops (Figure 1B, b and c) and the axoglial junction between the loops and the axolemma (Figure 1B, d and e) at paranodes and was present only occasionally in the paranodal axon (Figure 1B, d). These observations indicate that Nogo-A is a component of the CNS paranodes.

Nogo-A is a paranodal element predominantly derived from oligodendroglia

To characterize the cellular origin of the paranodal Nogo-A, we examined the distribution of Nogo-A in two animal models: experimental autoimmune encephalomyelitis (EAE), a condition exhibiting progressive CNS demyelination (Swanborg 2001), and $CGT^{-/-}$ mice known to display the presence of reversed lateral loops but an absence of transverse bands and abnormal localization of K^+ channels along their axons (Dupree *et al*., 1999). At the peak of demyelination in adult EAE rats, their longitudinal spinal cord sections were prepared for double immunofluorescence staining for Nogo-A or Caspr and for Kv1.1. The density of Nogo-A-positive paranodal congregates was significantly decreased (by around 90%) in sections from EAE rats (Figure 2A, a and c) compared with those from control animals. Only occasional foci of Nogo-A-positive paranodal clusters (arrowhead in Figure 2A, a) and oligodendroglial immunoreactivity remained (star in Figure 2A, a). In correlation with the loss of paranodal staining, the Nogo-A expression level in the spinal cord was downregulated in EAE rats (Figure 2A, d). However, Caspr expression was affected to a much lesser extent by this disorder in the spinal cord (Figure 2A, b–d).

In P16 wild-type mice, Nogo-A (green) clustered beside the congregated Na^+ channels (red) at paranodes (Figure 2B, a). However, in P16 $CGT^{-/-}$ mice, the correlation between the congregations of both Nogo-A (green) and Na^+ channels (red) was barely detected along the axons (Figure 2B, b). Double labeling of the 200 kDa neurofilament with Nogo-A revealed loose spiral-like labeling of Nogo-A along all of the neurofilament labeled axon in P21 $CGT^{-/-}$ mice (Figure 2B, d). This rather deranged labeling pattern was clearly different from the compact clustering pattern of Nogo-A labeling in wild-type animals (Figure 2B, a and c). The above results suggest that the Nogo-A clustering along the axon is severely disrupted in the mutants. IEM observations showed that Nogo-A immunoreactivity nevertheless remained detectable in the reversed lateral loops at paranodes in these mutant mice (Figure 2B, e and f). These results, which demonstrate loss of paranodal clustering of Nogo-A in both the EAE rat model and CGT mutant mice, attests to the notion that paranodal Nogo-A is present on oligodendrocytes.

Nogo-66 receptor NgR is not localized to the paranode

We next investigated the expression and distribution of the Nogo-66 receptor (NgR) to find out whether it also exhibits domain-specific congregation patterns in myelinated axons. Immunoblot analyses using NgR antibodies demonstrated that NgR expression was higher in adult brainstem, hippocampus and cerebral cortex, but was significantly lower in spinal cord (Figure 3A). NgR is detectable as early as postnatal day 1, with its expression level maintained until postnatal day 14 and subsequently showing a gradual decrease from 3 weeks of age (Figure 3B). To confirm that the NgR antibodies used could label NgR on neurons, we stained rat hippocampal sections and showed that NgR colocalized with the neuron-specific microtubule-associated protein 2 (MAP2) in cell bodies and processes (Figure 3C, D and E). Double labeling for NgR and Nogo-A was difficult because both antibodies originated from rabbits. Instead, we performed double labeling of NgR and Kv1.2. In longitudinal brainstem sections, NgR labeling clearly does not colocalize with the congregated K^+-channel labeling (Figure 3, F, G and H). Similar NgR labeling was observed at P1, P5, P14 and P30 sections (not shown). The observation that the NgR localization pattern is distinctly different from the congregated Nogo-A at the paranode raises the possibility that Nogo-A may interact with an axonal receptor other than NgR in these specific axon–glial domains.

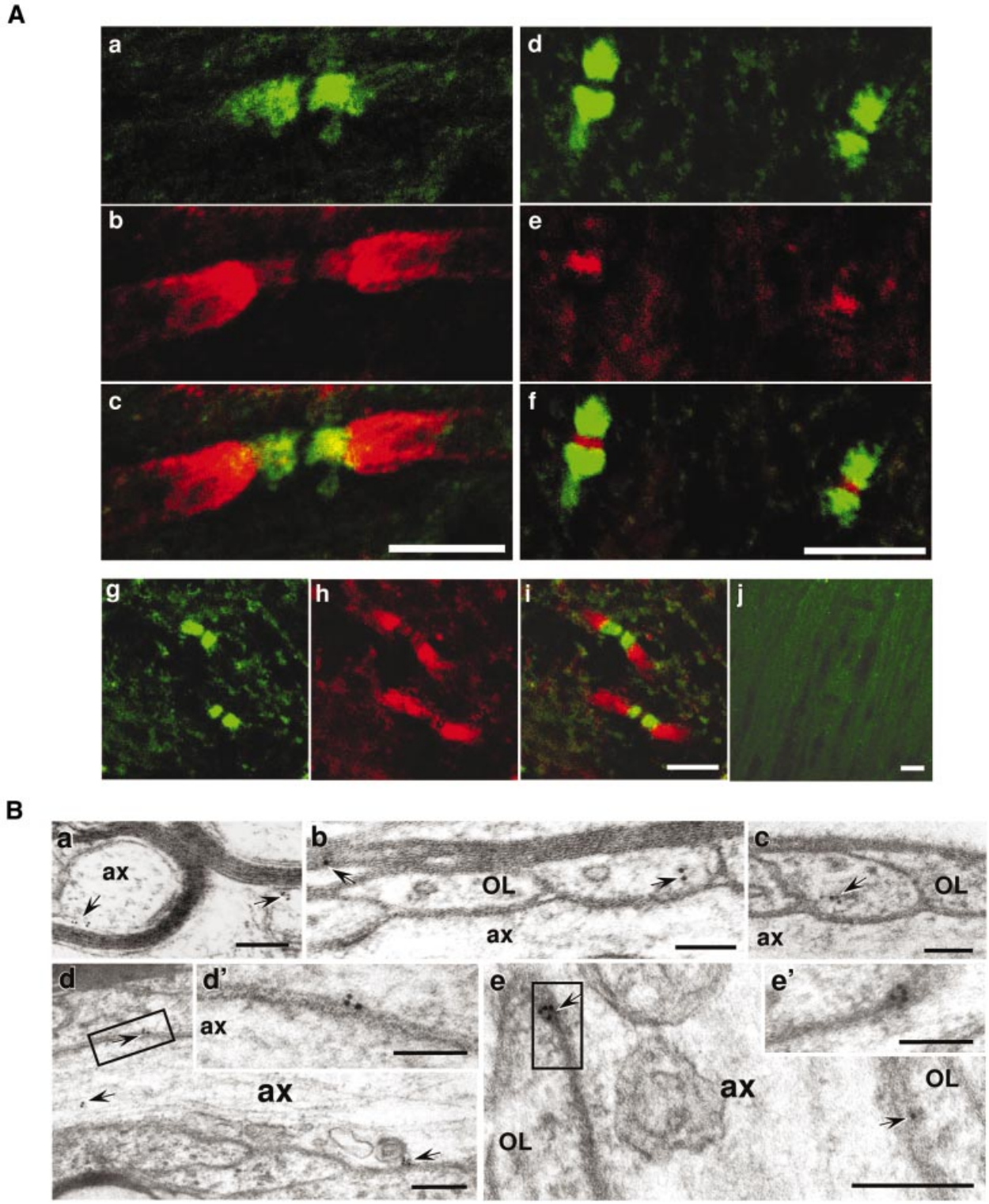

Fig. 1. Nogo-A clusters at the paranodes in the CNS. (**A**) Adult rat brainstem sections were double immunolabeled for Nogo-A (green: a, c, d, f, g and i) and the Kv1.1 K^+ channel α-subunit (red: b, c, h and i) or PAN Na^+ channel (red: e and f). For negative control, Nogo-A antiserum (1:200) was premixed with antigen before staining an adult brainstem section (j). Nogo-A antibodies used were those developed in our laboratory (a–f) or from Dr Strittmatter's laboratory (g–i). Images c, f and i are merged images of a and b, d and e, and g and h, respectively. (**B**) Ultrastructural localization of Nogo-A at the paranodes in rat spinal cord: (a) immunogold labeling of cross-sections of myelinated axons revealed that the gold particles were detected at the inner and outer myelin sheaths; (b and c) immunogold particles of Nogo-A are found within glial loops and the compacted myelin; (d and e) in longitudinal sections of paranodes, immunogold particles of Nogo-A located at the tips of glial loops in the axoglial junction and some within the axon in (d). The boxed areas in (d) and (e) are shown at higher magnification in (d′) and (e′).OL, oligodendrocyte; ax, axon. Gold particles are indicated with arrows. Scale bars: 5 μm for (A, a–i), 10 μm for (A, j), 200 nm for (B, a, d and e) and 100 nm for (B, b, c, d′ and e′).

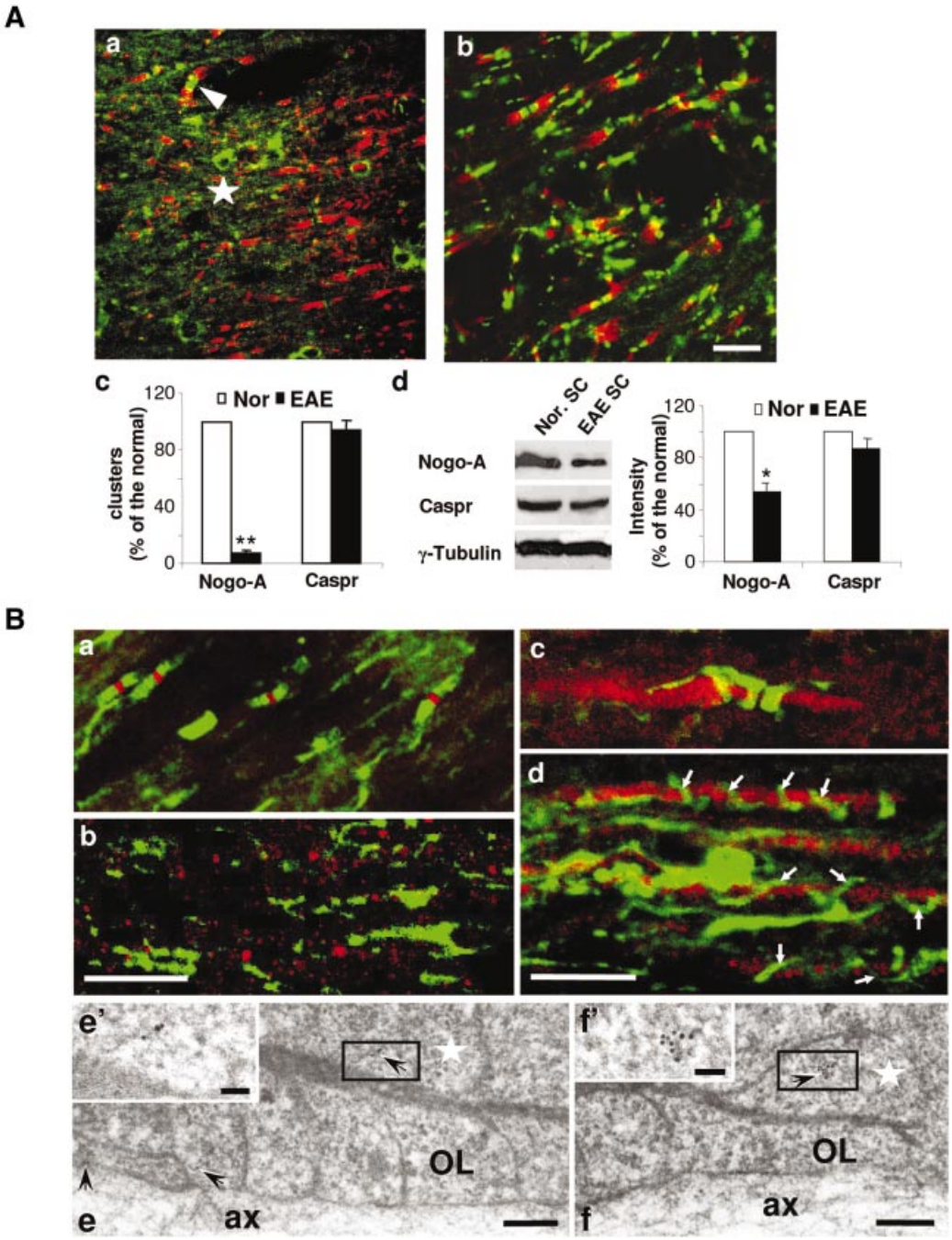

Fig. 2. Expression and localization of Nogo-A at the nodal areas in EAE rats and CGT$^{-/-}$ mice. (**A**) Expression and localization of Nogo-A and Caspr in EAE afflicted spinal cord. (a and b) Double immunostaining for Nogo-A (green, a), Caspr (green, b) and Kv1.1 (red, a and b). The star marks a Nogo-A-positive cell body and the arrowhead indicates an undisrupted paranodal Nogo-A labeling. (c) Numbers of Nogo-A and Caspr clusters in several microscope fields of both normal and EAE rat spinal cord sections were counted. Values are given as mean ± SEM from at least three independent experiments (** $P < 0.01$). (d) Western blotting results show that Nogo-A was significantly downregulated in the spinal cord of EAE animals, but Caspr expression was only affected slightly (* $P < 0.05$). Nor. SC, spinal cord of normal rats; EAE SC, spinal cord of EAE rats. Scale bars: 10 μm for (a) and (b). (**B**) Distribution of Nogo-A in spinal cord sections from wild-type and CGT$^{-/-}$ mice. (a and b) double labeling for Nogo-A (green) and Na^+ channel in wild-type and CGT$^{-/-}$ spinal cord (P16). In CGT$^{-/-}$ mice (b), the correlation between the congregations of both Nogo-A and Na^+ channels were barely detected compared with the wild-type sections (a), in which Nogo-A clustered at paranodes and Na^+ channels congregated at the nodes of Ranvier. (c and d) Spinal cord sections from wild-type and CGT$^{-/-}$ mice were double labeled for Nogo-A (green) and 200 kDa neurofilament (NF-200, red). Nogo-A labeling appears to be loosely spiraled around the axon in CGT$^{-/-}$ mice (P21; d), but clusters specifically into the paranodal region in wild-type mice (P21) (c). Arrows in (d) indicate the Nogo-A-labeled spirals. (e and f) Immunogold labeling of Nogo-A in longitudinal sections of paranodes from P16 CGT$^{-/-}$ mouse spinal cord demonstrated that gold particles were visible in the abnormally reversed loops. The boxed areas in (e) and (f) are shown at higher magnification in (e′) and (f′), respectively. Arrows indicate the 10 nm gold particles. Stars indicate the reversed papanodal loops. OL, oligodendrocyte; ax, axon. Scale bars: 10 μm for (a)–(d), 200 nm for (e) and (f), and 50 nm for (e′) and (f′).

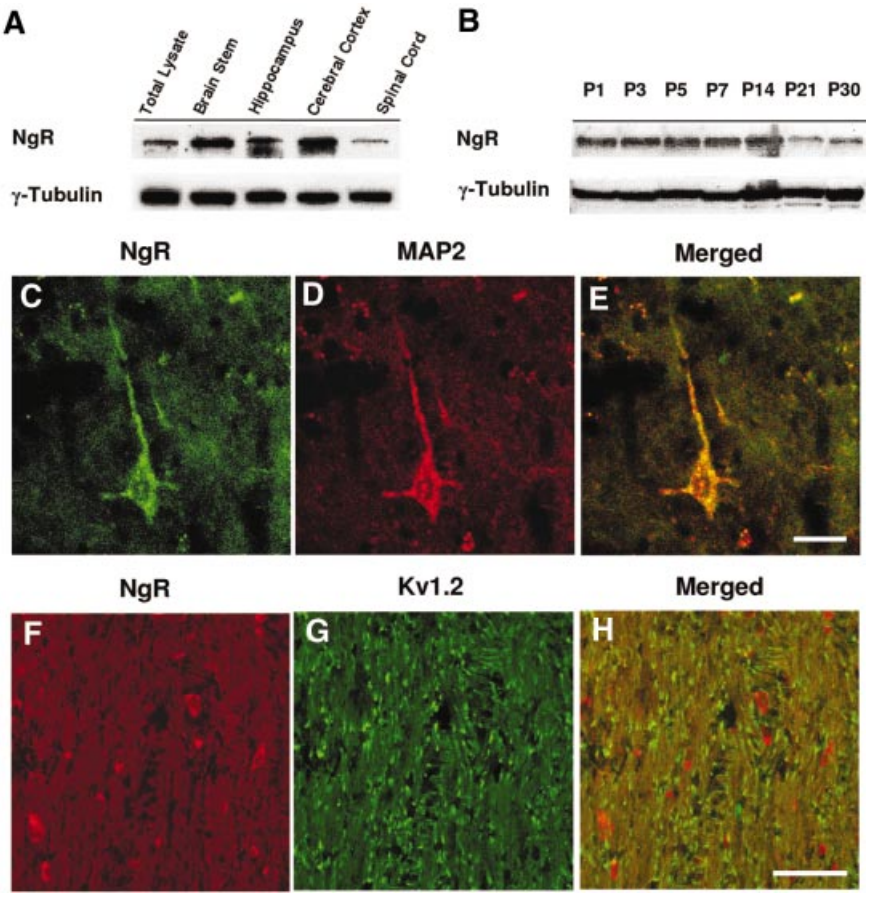

Fig. 3. NgR is not localized to the paranode. (**A** and **B**) Tissue lysates from various regions of the CNS of adult rats and brain lysates at various developmental stages were subjected to western blot using antibodies against NgR and γ-tubulin. (**C**–**E**) Adult hippocampus sections were double stained for NgR (green, C) and MAP2 (red, D). (E) is a merged image of (C) and (D). Scale bar: 10 μm. (**F**–**H**) Brainstem sections were double stained for NgR (red, F) and Kv1.2 (green, G). (H) is a merged image of (F) and (G). Scale bar: 50 μm.

Nogo-A interacts with paranodal Caspr–F3 complex

Given the paranodal location of Nogo-A, we investigated whether paranodal axonal components, such as Caspr, F3 and NB3 (an F3-related molecule) (Lee *et al*., 2000), are Nogo-A binding partners. Nogo-A, Caspr, F3 and NB3 were immunoprecipitated from membrane extracts of adult rat brain. Western blot analysis of the immunoprecipitates resolved by SDS–PAGE revealed that Nogo-A, Caspr and F3, but not NB3, were present in the immunocomplexes pulled down by either Nogo-A or Caspr antibodies (Figure 4A, a). Immunoprecipitation (IP) studies were also performed on Caspr–F3, F3 and wild-type CHO cells transiently transfected with a Nogo-A expression construct, as well as with Caspr–F3-CHO cells. Transfection was performed using Caspr–F3-expressing cells because F3 is required for coordinated cell surface expression of transfected Caspr (Faivre-Sarrailh *et al*., 2000). Western blotting demonstrated that Nogo-A and Caspr indeed associate with each other in Nogo-A–Caspr–F3 cells, but not Nogo-A–F3, Nogo-A or Caspr–F3 CHO cells (Figure 4A, b). These observations suggest that Nogo-A interacts specifically with Caspr rather than F3.

Nogo-A interacts directly in trans with Caspr via the extracellular Nogo-66 loop

The extracellular domain of Nogo-A consists of a 66 amino acid loop between its two transmembrane domains, known as the Nogo-66 domain (Fournier *et al*., 2001). Any interaction *in trans* between Nogo-A and Caspr should involve the Nogo-66 domain. We next investigated whether the Nogo-A and Caspr associate directly in a *trans* manner that is independent of F3 using a cell adhesion assay. Different CHO cell lines (expressing Caspr or otherwise) were plated onto substrates coated with the Nogo-66 peptide or recombinant GST fusion proteins containing Nogo-66 (GST–Nogo-66) or the cytoplasmic N-terminal domain of Nogo-A (GST–Nogo-N) as well as GST. Caspr–F3-expressing cells, but neither F3-expressing nor wild-type CHO cells, adhered readily to Nogo-66 (Figure 4B, a, b and c) or GST–Nogo-66 (Figure 4B, e–g). None of these CHO cell types adhered well to GST (Figure 4B, i–k) or GST–Nogo-N (not shown). Quantification of adhering cells indicated that the number of Caspr–F3-CHO cells binding to both Nogo-66 and GST–Nogo-66 was much higher than that in the other experimental groups (Figure 4B, m).

To investigate whether Nogo-66 interacts with Caspr only or with a binding pocket generated by the cell surface Caspr–F3 complex, we removed the GPI-linked F3 using phosphatidylinositol-specific phospholipase C (PI-PLC). After a PI-PLC treatment, Caspr–F3-CHO cells still adhered to both Nogo-66 and GST–Nogo-66, but not to GST-coated substrates (Figure 4B, d, h, l and m). To ensure that F3 was completely removed from the cell

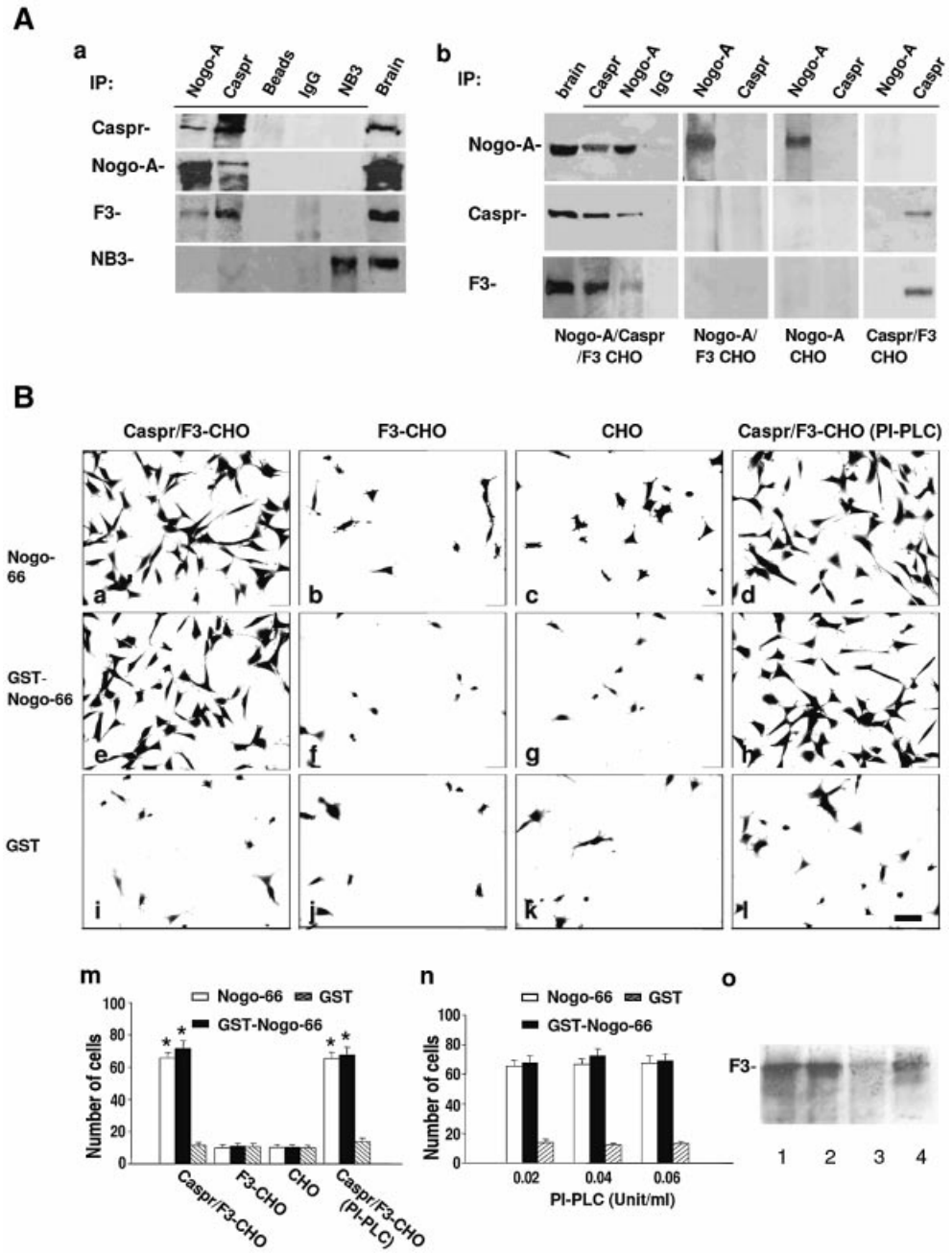

Fig. 4. Caspr associates with Nogo-66 in an F3-independent manner. (**A**) Nogo-A associates *in vivo* with Caspr–F3. (a) Detergent lysates of brain membrane fractions from adult mice were immunoprecipitated with Caspr, Nogo-A and NB3 antibodies as well as non-immune IgG. The immunoprecipitates and detergent extracts from brain (Brain) together with the protein-A beads (Beads) were subjected to western blot using antibodies against Caspr, Nogo-A, F3 and NB3. (b) Membrane fractions of Nogo-A–Caspr–F3-, Nogo-A–F3-, Nogo-A- and Caspr–F3-transfected CHO cells were immunoprecipitated with antibodies to Caspr and Nogo-A as well as non-immune IgG. The immunoprecipitates and brain extracts (Brain) were subjected to western blot analysis using antibodies against Nogo-A, Caspr and F3. (**B**) Caspr-expressing cells adhere to Nogo-66. (a–l) Caspr–F3-CHO cells (a, e and i), F3-CHO cells (b, f and j) and mock CHO cells (c, g and k), as well as PI-PLC-treated Caspr–F3- CHO cells (d, h and l) were plated onto substrates coated with Nogo-66 peptide, recombinant GST–Nogo-66 protein and GST, respectively. Scale bar: 8 μm. (m and n) Quantification of cells adherent to various substrates. Caspr–F3-CHO cells (in the presence or absence of PI-PLC treatment), but neither F3-CHO nor wild-type CHO cells, bound to Nogo-66 peptide and GST–Nogo-66. Bars represent the number of adherent cells (expressed as mean ± SEM) from at least three independent experiments (m). (o) At the end of cell adhesion assay after PI-PLC treatment, Caspr–F3-CHO and F3-CHO cells and their culture supernatant were collected and subjected to western blotting analysis after normalizing for total protein to detect F3/contactin: 1, mouse brain; 2, F3-CHO cell lysate; 3, Caspr–F3-CHO cell lysate after PI-PLC treatment; 4, Caspr–F3-CHO cell medium after PI-PLC treatment. *$P < 0.05$. Caspr–F3- CHO cells adhered to Nogo-66 and GST–Nogo-66 with equal efficiency after treatment with increasing concentrations of PI-PLC (0.02, 0.04 and 0.06 U/ml) (n).

surface after PI-PLC treatment, increasing concentrations of PI-PLC (0.02, 0.04 and 0.06 U/ml) were used. The level of cell binding was constant in all three different concentrations of PI-PLC (Figure 4B, n). In agreement with our previous work (Faivre-Sarrailh *et al.*, 2000), western blot (Figure 4B, o) and immunostaining (not shown) using F3 antibodies demonstrated that a significant amount of F3 was indeed removed from Caspr–F3-CHO

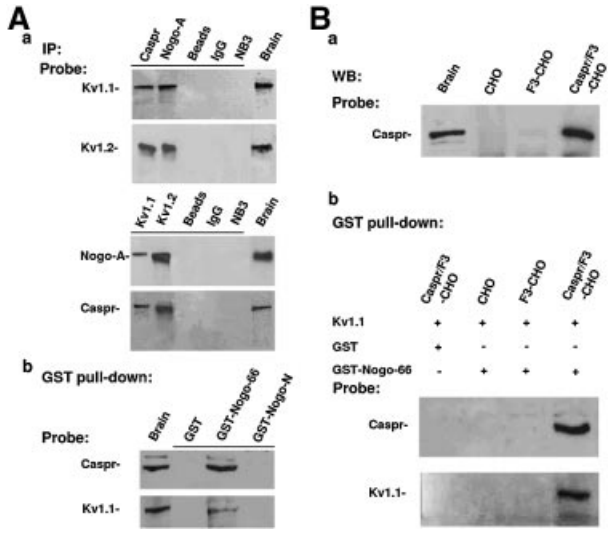

Fig. 5. The Nogo-A–Caspr complex interacts with K^+ channels. (**A**) (a) P7 mouse brain membrane extracts were immunoprecipitated with Caspr, Nogo-A, Kv1.1, Kv1.2 and NB3 antibodies as well as non-immune IgG. The indicated immunoprecipitates and brain extracts (Brain) were subjected to western blot analysis using antibodies against Kv1.1, Kv1.2, Nogo-A and Caspr. (b) GST pulldown assay was performed using recombinant GST–Nogo-66, GST–Nogo-N and GST from adult mouse brain extracts. The indicated precipitates and brain extracts (Brain) were probed with Caspr and Kv1.1 antibodies, following SDS–PAGE separation. (**B**) (a) Membrane fraction of CHO, F3-CHO and Caspr–F3 CHO cells, as well as brain extracts, were immunoblotted using Caspr antibodies following SDS–PAGE separation. (b) After transient transfection with the Kv1.1 expression construct RBG4/Kv1.1, membrane extracts of CHO, F3-CHO and Caspr–F3 CHO cells were incubated with GST–Nogo-66 or GST, respectively. The eluted proteins were separated by SDS–PAGE and probed with Caspr and Kv1.1 antibodies. IP, immunoprecipitation; WB, western blot.

cells after treatment with PI-PLC. This lack of effect of PI-PLC on the cell adherence to Nogo-66 substrates suggests that F3 is not directly involved in the *trans* interaction between Nogo-66 and Caspr.

The Nogo-A–Caspr complex interacts with K^+ channels

During myelination, the proper segregation of K^+ channels to juxtaparanodes requires an intact paranodal axoglial junction (Vabnick and Shrager, 1998). This structure is formed and maintained by axonal molecules such as Caspr and F3, as well as by glial-specific molecules during myelination and remyelination (Girault and Peles, 2002). We hypothesized that the interaction of Nogo-A with Caspr forms an axoglial signaling connection that could influence the final location of the K^+ channel at juxtaparanodes during the early stages of myelination. Immunoprecipitation analyses were performed to investigate whether K^+ channels could physically interact with Nogo-A–Caspr complex in the CNS. Both Nogo-A and Caspr antibodies reciprocally precipitated Kv1.1 and Kv1.2, but not Kv2.1 (not shown), from P7 and adult (not shown) mouse brain extracts, while NB3 antibody and non-immune IgG did not (Figure 5A, a). Kv2.1 is generally found in neuronal cell bodies and proximal dendrites, but is excluded from axons (Trimmer, 1991). In GST pulldown assays using membrane extracts of adult mouse brain, both Caspr and Kv1.1 could be pulled down by GST–Nogo-66, but not by GST–Nogo-N or GST (Figure 5A, b). These results support the notion that Nogo-66 is a *trans*-interacting partner of Caspr and that K^+ channels may interact with the complex.

Nogo-66 interacts indirectly with K^+ channels via Caspr

We next asked whether Nogo-66 could directly interact with K^+ channels. Kv1.1 cDNA (Nakahira *et al*., 1996) was transiently transfected into Caspr–F3, F3 and wild-type CHO cells and the membrane extracts were subjected to a GST pulldown assay using GST and GST–Nogo-66 fusion proteins, respectively. Wild-type and F3-expressing CHO cells did not express Caspr (Figure 5, Ba). Western blot analysis showed that both Kv1.1 and Caspr could be precipitated by GST–Nogo-66, but not by GST, from the Caspr–F3-expressing cells, but not from F3-expressing and wild-type CHO cells (Figure 5B, b). These results demonstrate that Nogo-66 could interact indirectly, at least *in vitro*, with K^+ channels via Caspr.

Nogo-A and Caspr share a similar spatial and temporal relationship with Kv1.1 along myelinated axons during development

In view of the potential interaction between the paranodal Nogo-A–Caspr and Kv1.1 established above, we explored the dynamic relationship between Nogo-A–Caspr and Kv1.1 distribution along myelinated axons during development. Double immunofluorescence labelings of Caspr and Kv1.1, and of Nogo-A and Kv1.1, were performed on brainstem sections of rats at various postnatal ages. Congregations of both Caspr and Kv1.1 labeling were apparent from approximately P5 onwards (Figure 6A, a). From P5 to P14 (Figure 6A, a–c), Caspr staining at paranodes overlapped that of Kv1.1, suggesting colocalization of both molecules at this critical early period of myelination. At P30 (Figure 6A, d), Kv1.1 labeling became more distinctly juxtaparanodal, with only minimal bands of overlap with Caspr at paranodal–juxtaparanodal borders. In the adult (Figure 6A, e), Caspr and Kv1.1 were segregated into their different microdomains along the myelinated axons. Double immunofluorescence staining for Nogo-A and Kv1.1 at P1 (Figure 6B, a–c) revealed that Nogo-A was diffusely labeled along the nerve fibers. At P5 (Figure 6B, d–f), clustering and aggregation of Nogo-A staining became more evident. However, the staining pattern still did not have well-defined domains or borders. Nodal gaps were apparent and heminodes were seen as well. From P7 onward (Figure 6B, g–i), Nogo-A distribution demonstrated an obvious clustering toward the paranodes. Between P5 and P14 (Figure 6B, j–l), there were varying degrees of overlap between congregates of Nogo-A and Kv1.1 immunostaining at both paranodal and juxtaparanodal regions. At P30 (Figure 6B, m–o), Kv1.1 congregates were exclusively localized to juxtaparanodes, akin to the situation in adult animals.

Colocalization of the Nogo-A–Kv1.1 and Caspr–Kv1.1 was quantified by measuring the lengths of Nogo-A and Kv1.1-labeled regions on captured images (Figure 6C, a). The average length of a Nogo-A-labeled region was about 9 μm at P5 and 5 μm at P7, but this shortened to about 2 μm from P14 to adult, suggesting that Nogo-A is progressively

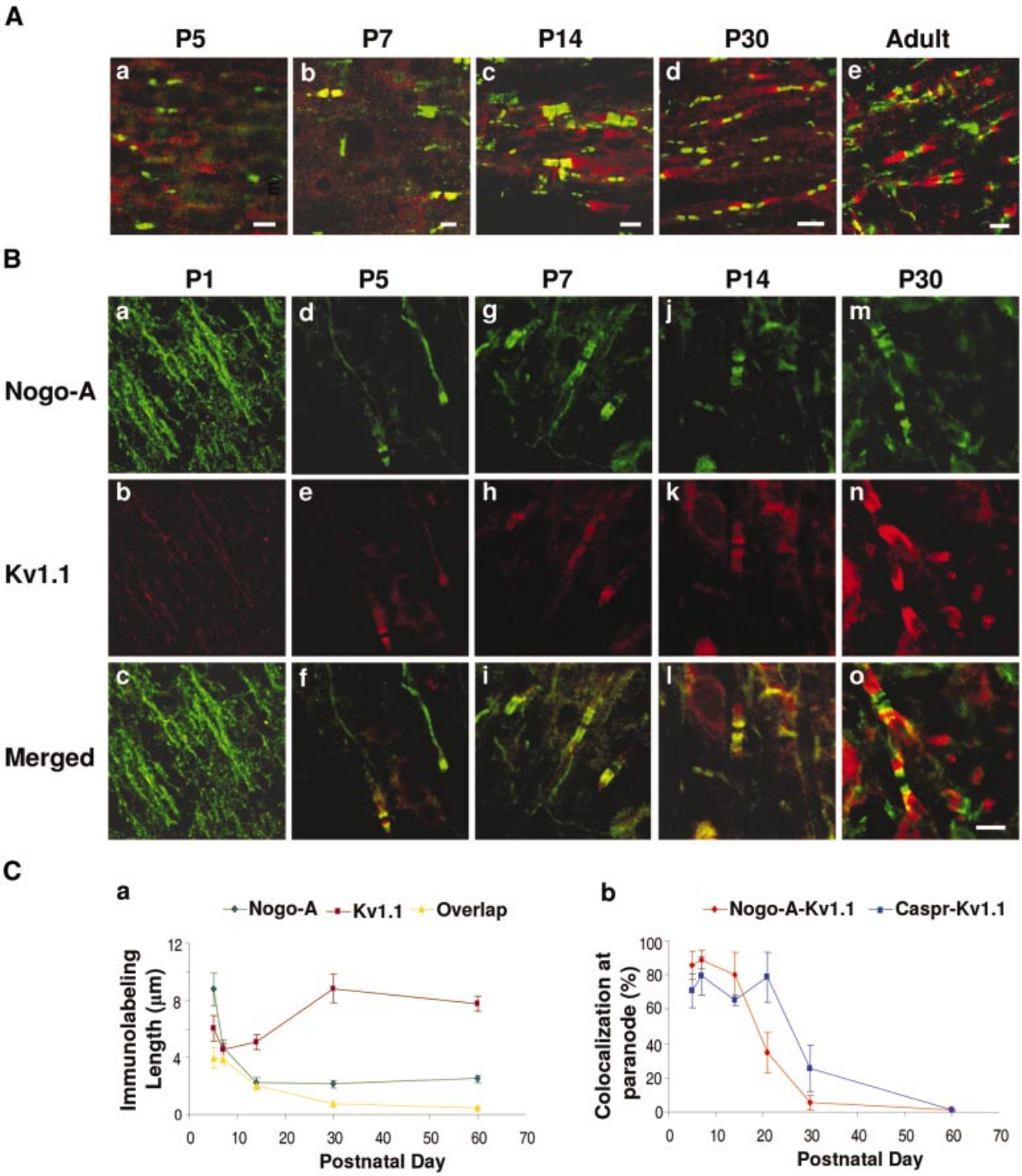

Fig. 6. Immunohistochemical labeling of Nogo-A, Caspr and Kv1.1 at different postnatal days in rat brainstem. (**A**) Brainstem sections of P5 to adult rats were double labeled for Caspr (green) and Kv1.1 (red). Scale bar: 5 μm. (**B**) Sections from P1–P30 rats were double labeled for Nogo-A (green) and Kv1.1 (red). Scale bar (o): 5 μm. (**C**) (a) The lengths of Nogo-A and Kv1.1 immunostaining and their overlap were measured from micrographs (μm, mean ± SEM). (b) The number of overlapping Nogo-A–Kv1.1 or Caspr–Kv1.1 clusters at paranodes was counted.

congregated into narrower bands during the early stages of myelination. The average length of a Kv1.1-labeled region did not demonstrate such a marked change with time, ranging from 6 μm at P5 to 8 μm in the adult. Of note was the change in terms of the length of overlap between Nogo-A and Kv1.1 labeling: it decreased from 4 μm at P5, 2 μm at P14 and 1 μm at P30 to approximately 0 μm in the adult. This change demonstrates a transient colocalization of Nogo-A and Kv1.1 in paranodal regions before compact myelin is fully laid down. The degree of colocalization between Nogo-A–Kv1.1 and Caspr–Kv1.1 was also compared (Figure 6C, b). From P5 to P14, >60% of paranodes in every field of view were double labeled for Nogo-A–Kv1.1 and Caspr–Kv1.1, respectively. In adults, Nogo-A and Caspr separated from Kv1.1 and a complete segregation was observed. Given that K^+ channels bind to the

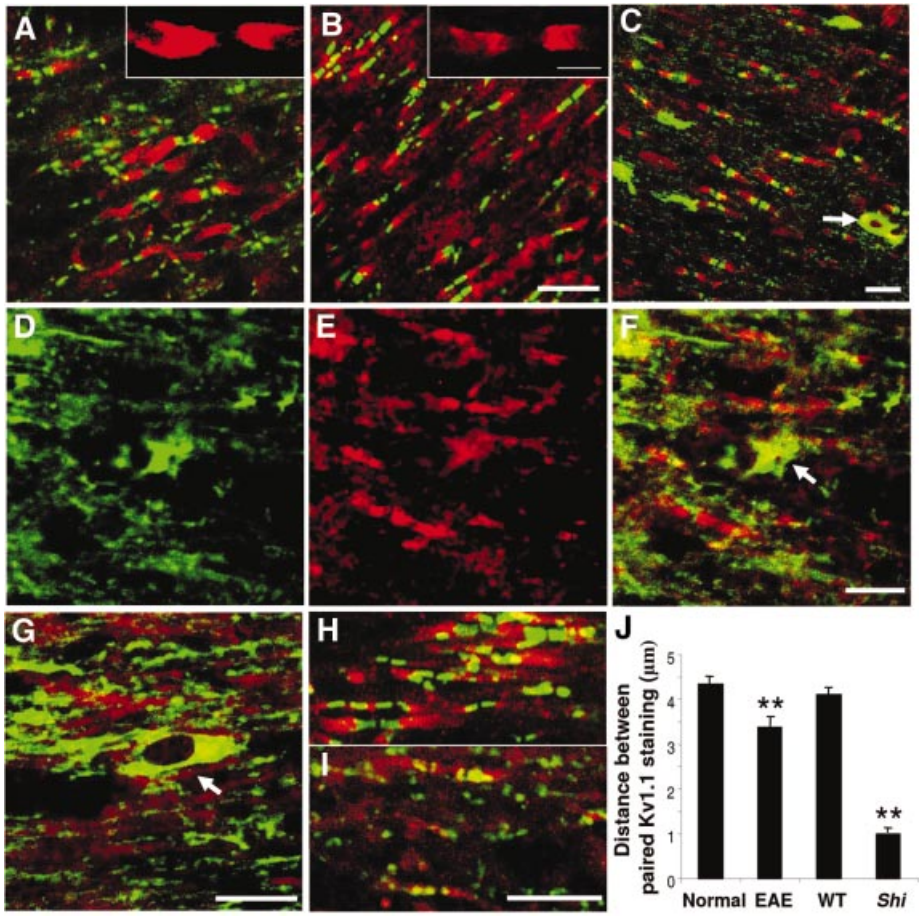

Fig. 7. Distribution of Nogo-A, Caspr and Kv1.1 in EAE rats and *Shiverer* mice. (**A** and **B**) Double immunofluorescence labeling for Caspr (green) and Kv1.1 (red) in brainstem sections of (A) EAE and (B) control rats. The insets represent magnified views of the Kv1.1 labeling. Scale bars: 10 μm for (A) and (B), and 5 μm for insets to (A) and (B). (**C**, **D**, **E**, **F** and **G**) Double labeling for Nogo-A (green) and Kv1.1 (red) in spinal cord sections of (C) wild-type and (D–G) *Shiverer* mice. Image (F) is a merged image of (D) and (E). Arrows in (C), (F) and (G) indicate Nogo-A-positive cell bodies. Scale bars: 10 μm. (**H** and **I**) Double immunofluorescence staining of Caspr (green) and Kv1.1 (red) in brainstem sections of (H) wild-type and (I) *Shiverer* mice. Scale bar: 10 μm. (**J**) The distances between paired Kv1.1 staining in EAE with control rats and *Shiverer* (*Shi*) with wild-type (WT) mice were measured from micrographs (μm, mean ± SEM), respectively. The values in EAE rats or *Shiverer* mice were significantly reduced when compared with their controls, respectively (**$P < 0.01$).

Nogo-A–Caspr complex, these observations imply that the Nogo-A–Caspr complex may transiently interact with K^+ channels, and as such may cooperatively regulate the paranodal localization of Kv1.1 during the early stages of myelination.

Nogo-A and K^+ channel in demyelinating animal models

Shiverer is a hypomyelinating mutant mouse that lacks myelin basic protein (MBP) and has axons with normal oligodendroglial ensheathment, but displays aberrant axoglial junctions and abnormal localization of K^+ channels along its axons (Rasband and Trimmer, 2001). To explore the spatial relationship between glia-related molecules and K^+ channels in myelinated axons, the distribution of Nogo-A, Caspr and Kv1.1 was examined in both rats subjected to EAE and *Shiverer* mice. Double-immunofluorescence staining demonstrated that both disorganized Caspr (green) and Kv1.1 (red) labelings were detectable in the paranodal regions of the EAE rat (Figure 7A) compared with normal rat (Figure 7B) brainstem. In contrast with the location of paranodal Nogo-A (green) and juxtaparanodal Kv1.1 (red) in the spinal cord sections of normal mice (Figure 7C), Nogo-A clustering was barely detectable in the paranodal region of *Shiverer* mice (Figure 7D, E, F and G). However, Nogo-A immunoreactivity in cell bodies remained intact and distinct (arrows in Figure 7C, F and G). In accordance with previous observations (Poliak *et al*., 2001), disorganized Caspr and Kv1.1 labeling colocalized at paranodes in *Shiverer* mice (Figure 7I) but not in normal mice (Figure 7H). Quantitative analysis of the distance between paired Kv1.1 immunostainings demonstrated that the distances between the pairs were significantly reduced in both EAE and *Shiverer* mice compared with normal animals ($P < 0.01$) (Figure 7J). These observations suggest that, in both pathological conditions of EAE rats and *Shiverer* mice displaying paranodal junction defects, K^+ channels are relocated to the paranodes. Concomitantly, the congregation of Nogo-A at the paranode was markedly reduced. Thus, in addition to axonal molecules, certain glia-derived molecules involved in formation of axoglial junctions may also be essential for proper K^+-channel localization at juxtaparanodes in normal adult animals.

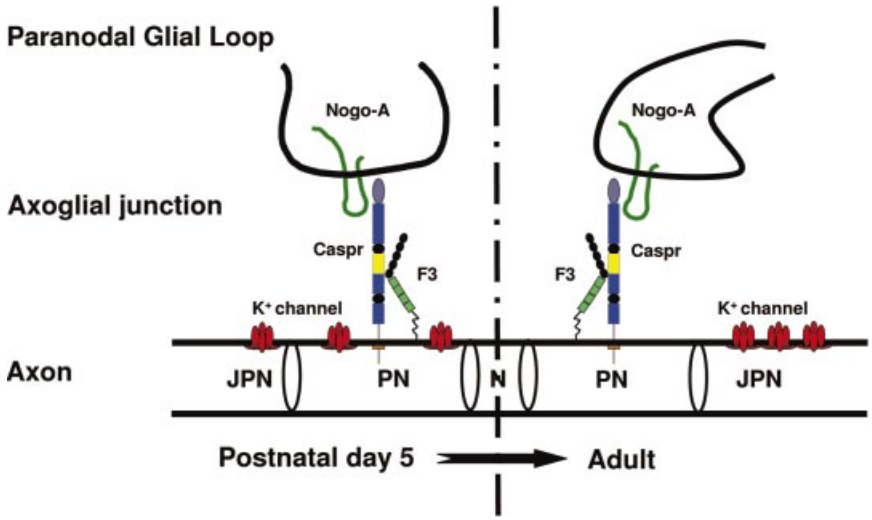

Fig. 8. The interaction between Nogo-A and Caspr at the paranodes may play a role during myelination. Paranodal Nogo-A *trans* interacts with axonal Caspr and may play a role in K^+-channel localization during the early stages of myelination (from P5). With the firm establishment of axoglial junctions in the adults, K^+ channels were excluded from paranodes where Nogo-A–Caspr interaction is maintained. The mechanisms for this separation remain to be further explored. N, node of Ranvier; PN, paranode; JPN, juxtaparanode.

The molecular structural basis for these changes is presently unknown, but may well be related to the interaction between K^+ channels and the Nogo-A–Caspr complex.

Discussion

Nogo-A, but not the Nogo-66 receptor, is located at the paranode

In the present study, we have first investigated whether glia-derived Nogo-A is specifically localized to distinct axonal domains, such as paranodes, and as such may be involved in intercellular axoglial signaling. Nogo-A is localized to oligodendrocyte cell bodies and processes and to the innermost loop and outer loop of the myelin sheath (Huber *et al*., 2002). During development, the time course of appearance of Nogo-A mRNA and protein parallels the time frame for myelination, occurring in a period just prior to the expression of myelin basic protein (Huber *et al*., 2002). We show that Nogo-A is mainly localized at the gaps between Na^+ and K^+ channels along axons and its immunoreactivity is clearly located at sites where glial loops make contact with the axonal membrane surface in adult CNS. In accordance with Nogo-A downregulation, its congregates are significantly reduced at paranodes in EAE animals. Although Nogo-A immunoreactivity remains detectable at the abnormal glial loops of $CGT^{-/-}$ mice on ultrastructural analysis, immunohistochemical examination of axons in both *Shiverer* and $CGT^{-/-}$ mice revealed a loss of paranodal clustering of Nogo-A. Together, these observations support the notion that Nogo-A is a paranodal glial component (Figure 8).

The staining pattern and oligodendroglial origin of paranodal Nogo-A raises the question as to whether it interacts with components on the axonal surface. So far, NgR is the only known high-affinity neuronal receptor for Nogo-A. NgR expression in neurons and along myelinated axons is predominantly found in adult animals and is minimal during myelination (McGee and Strittmatter, 2003). Consistent with these findings, we have shown that NgR is located in the brainstem on neuronal cell bodies and uniformly distributed along myelinated axons from the early stages of development until adulthood. It is intriguing that there is significant Nogo-A clustering at paranodes, while the NgR distribution pattern remains diffuse along axons. Therefore, as the congregation of Nogo-A coincides with the developmental period of myelination, paranodal Nogo-A may participate in this process and may interact with a molecule other than NgR for a function distinct from inhibition of axonal sprouting.

Paranodal Nogo-A is a trans-binding partner of Caspr

At the paranodes, the GPI-anchored axonal F3/contactin exists as a complex with the membrane protein Caspr (Girault and Peles, 2002). The Caspr–F3 complex interacts with NF155, a glial-derived molecule, *in trans*, and is an example of axoglial molecular connection at the paranode (Girault and Peles, 2002). We have shown that Nogo-A associates specifically with the Caspr–F3 complex, but not with NB3, another paranodal molecule (Ang *et al*., 2001), in co-immunoprecipitation assays, implicating an interaction between Nogo-A and the complex *in vivo*. The observation that the majority of CNS Nogo-A is detected in oligodendroglial cytoplasm and in the reversed paranodal lateral loops from $CGT^{-/-}$ mice implies that this interaction probably occurs in a *trans* manner, with Nogo-A from the oligodendrocyte membrane interacting with Caspr–F3 from the axonal membrane. Although it remains a possibility that axonal Nogo-A is a *cis*-binding partner in the Caspr–F3 complex, and is dependent upon myelination for congregation, this seems unlikely since paranodal Nogo-A is predominantly expressed by oligodendrocytes in the CNS (Huber *et al*., 2002; Liu *et al*., 2002; Wang *et al*., 2002). We showed that Caspr–F3-expressing CHO cells bind to both substrates coated with

Nogo-66 peptides and GST–Nogo-66, where the binding must occur in a *trans* manner. That binding occurs even after removal of F3 from the cells via PI-PLC treatment further implies that Nogo-A interacts directly with Caspr (Figure 8).

Nogo-A may complement Caspr in regulating Kv1.1 location

There is strong evidence suggesting that K^+-channel accumulation at the juxtaparanode is influenced by myelinating oligodendrocytes (Vabnick and Shrager, 1998). In the myelinated axons of the CNS, K^+-channel labeling becomes more prominent during the progression of postnatal development, initially localizing to juxtaparanodes and also to paranodal bands that alternate with Caspr immunoreactivity (Rasband *et al*., 1999). At later stages of postnatal development, K^+ channels are excluded from the paranodes and become exclusively juxtaparanodal. We showed that Nogo-A, via Caspr, associates indirectly with Kv1.1. In addition, the developmental changes in the distribution pattern of Nogo-A and Kv1.1, as well as in those of Caspr and Kv1.1, are similar, implying that an interaction between Kv1.1 and the Nogo-A–Caspr complex may occur, at least transiently, when Nogo-A–Caspr colocalizes with Kv1.1 at paranodes during the early stages of myelination. Therefore Nogo-A may complement or regulate the action of Caspr in the organization of mature axonal domains and in so doing aid in the coordinated localization of K^+ channels to juxtaparanodes (Figure 8). Investigation of Nogo-A (or Nogo-A–Caspr) constitutive or conditional deficient animals *in vivo*, possibly using oligodendrocyte-specific promoters, may help to reveal further the role of Nogo-A during myelination. According to our quantitative analyses in both EAE rats and *Shiverer* mice, the lengths of the gaps between paired K^+-channel clusters were reduced significantly. This occurred in conjunction with a significant reduction in Nogo-A clusters. Therefore K^+ channels may colocalize with Caspr again in these pathological conditions. It will be interesting to explore whether this transient interaction also occurs during remyelination.

It should be noted that the localization of Caspr family members demarcates distinct domains in myelinated axons. Caspr2, which is about 45% identical to Caspr, is localized to the juxtaparanodes of adult myelinated axons. It associates with K^+ channels indirectly via its C-terminus, which contains a putative PDZ binding site (Poliak *et al*., 1999), a feature shared by two other recently described members of the mammalian Caspr family, Caspr3 and Caspr4 (Spiegel *et al*., 2002). The C-terminus of Caspr is rather unique compared with other members of the family in terms of its length, and the antibody we have raised is unlikely to cross react with the other Caspr isoforms. The C-terminus of Caspr does not have a putative PDZ binding motif, but shares a band 4.1 binding domain with Caspr2 (Scherer and Arroyo, 2002). It would be interesting to determine whether this domain of Caspr mediates its interaction with Kv1.1 and Kv1.2.

Nogo-A interactions in the CNS

The only known interacting partners of Nogo-A, other than NgR, are the Nogo-interacting mitochondrial protein (NIMP) (Hu *et al*., 2002), α-tubulin and MBP (Taketomi *et al*., 2002). Our results indicate that the cell-surface-exposed Nogo-66 loop binds directly to Caspr at axonal surface, thus highlighting a previously unsuspected function of Nogo-A at the axoglial junction. This interaction does not appear to involve NgR. In fact, it is unclear whether interactions between adult oligodendroglial Nogo-A and axonal NgR are required under normal physiological conditions. Although further studies are required to determine the precise function of the Nogo-A–Caspr interaction, we postulate that this may in some manner shape and maintain the architecture of the axoglial junctions during and after myelination (Figure 8). The Nogo-A–Caspr interaction represents the first NgR-independent Nogo-66 interaction described to date, and has significant implications for the role of Nogo-A in formation and maintenance of the axoglial junction architecture.

Materials and methods

Materials

Polyclonal Nogo-A (Liu *et al*., 2002; Wang *et al*., 2002), NgR (Wang *et al*., 2002), F3 (Shimazaki *et al*., 1998) and NB3 (Lee *et al*., 2000) antibodies have been described previously. Kv1.1, Kv1.2 and Kv2.1 antibodies (Chemicon), monoclonal antibody against Kv1.1 α-subunit (K20/78), Kv1.2 α-subunit (K14/16, Upstate), Na^+ channel (K58/35), NF-200 and MAP2 (Sigma) are from the respective commercial sources. Polyclonal NgR and Caspr antibodies were obtained by immunization of rabbit with a GST fusion protein to amino acids 277–430 of human NgR and to amino acids 1308–1377 of human Caspr, respectively.

Nogo-66 peptide (KLSDVLDDVLFLRRLEKITCNVHGLASNSYKQVLEES IAVESELYARFPHGEDSKQIAQIVGKYIR) was from oke Diagnostics ApS (Denmark). Recombinant GST–Nogo-66 and GST–Nogo-N-terminal (GST–Nogo-N) were amplified from human brain cDNA clone HK07722 (Nogo-A) by PCR.

EAE model

The EAE model in rats was developed according to a previous report (Ahn *et al*., 2001). At 13–14 days post-myelin extract injection (dpi), animals at the peak stage of EAE were sacrificed for further experiments.

Immunohistochemistry and immunoelectron microscopy

Wistar rats, $CGT^{-/-}$ mice (Coetzee *et al*., 1996) and *Shiverer* mice (adults, Jackson Laboratories, Bar Harbor, ME) were perfused, and spinal cords and brainstems were post-fixed in 4% paraformaldehyde for 2 h and processed for immunohistochemistry as previously described (Huber *et al*., 2002). For electron microscopy, samples from adult Wistar rats and $CGT^{-/-}$ (P16) were prepared according to published protocols (Huber *et al*., 2002) and examined under a Philips 208 electron microscope.

Western blot, co-immunoprecipitation and GST pulldown assays

Various regions of the CNS (total brain, brainstem, hippocampus, cerebral cortex and spinal cord) from adult (P1–P30) Wistar rats and spinal cords from EAE and control rats were harvested and extracted in phosphate-buffered saline containing 1% Triton X-100 and a cocktail of protease inhibitors. Lysates were electrophoresed on SDS–PAGE gel and blotted onto nitrocellulose membranes (Hybond C-extra, Amersham). Identical blots were probed with antibodies against Nogo-A, Caspr, NgR and γ-tubulin (for loading normalization) and visualized with the Pierce chemiluminescent detection reagents.

For co-immunoprecipitation and GST pulldown experiments, brain or cell membrane fractions were prepared as described previously (Lei *et al*., 2002). Briefly, brain tissue or cells were homogenized in ice-cold homogenizing buffer (320 mM sucrose, 10 mM Tris–HCl pH 7.4, 1 mM $NaHCO_3$ pH 7.4, 1 mM $MgCl_2$) supplemented with 1% protease inhibitor cocktail (Amersham) and subsequently centrifuged at 5000*g* for 15 min. The supernatant was collected and spun at 60 000*g* (Beckman ultracentrifuge) for 60 min at 4°C. Pellets were then dissolved in a lysis buffer (10 mM Tris–HCl pH 9, 150 mM NaCl, 0.5% Triton X-100, 1% sodium deoxycholate, 0.5% SDS, 2 mM EDTA and 1% protease inhibitor cocktail). The sample was preincubated with non-immune rabbit IgG and

protein-A agarose or the bead-bound GST, GST–Nogo-66 and GST–Nogo-N (20 μg) before the subsequent experiments.

In separate experiments, Nogo-A or Kv1.1 (Nakahira *et al*., 1996) expression constructs in the mammalian expression vector were transiently transfected into Caspr–F3-expressing CHO (Faivre-Sarrailh *et al*., 2000), F3-expressing CHO (Gennarini *et al*., 1991) or wild-type CHO cells for co-immunoprecipitation and GST pulldown studies.

Cell adhesion assay

The cell adhesion assay was carried out as previously described (Xiao *et al*, 1996).

PI-PLC treatment

Where indicated, Caspr–F3-transfected CHO cells were treated with PI-PLC (0.02, 0.04 or 0.06 U/m) (Sigma), incubated for 2 h and then plated into the dishes for cell adhesion assays or subjected to western blot analysis and immunocytochemistry for F3/contactin as mentioned above.

Acknowledgements

We sincerely thank Dr Malcolm Paterson (Singapore Health Service Pte Ltd, Singapore) for insightful comments and revision of the manuscript. We thank Dr Stephen Strittmatter (Yale University School of Medicine) for providing the NgR and Nogo-A antibodies, and for his kind advice and critical discussions. We are grateful to Dr James S.Trimmer (State University of New York) for the gift of RBG4/Kv1.1. We thank Haiping Liu and Belinda Ling for technical assistance. This work was supported by grants from the National Medical Research Council of Singapore, Singapore Health Service Pte Ltd and Department of Clinical Research, Singapore General Hospital to Z.C.X., the Association pour la Recherche sur la Sclerose en Plaques to C.F.-S., the Institute of Molecular and Cell Biology from the Agency for Science, Technology and Research of Singapore to B.L.Tang (a cross appointee of the Office of Life Sciences, National University of Singapore), the Agency for Science, Technology and Research, Singapore and the Canadian Institutes of Health Research to C.J.P., the Hertie Foundation and the European Union to M.S., and the NIH (NS27336) to B.P.

References

Ahn,M., Min,D.S., Kang,J., Jung,K. and Shin,T. (2001) Increased expression of phospholipase D1 in the spinal cords of rats with experimental autoimmune encephalomyelitis. *Neurosci. Lett.*, **316**, 95–98.

Ang,B.T. *et al*. (2001) Notch is a receptor for F3/contactin and NB-3: a paranodal axon-glial signaling mechanism during myelination. *Abstr. Soc. Neurosci.*, 900.5.

Bhat,M.A. *et al*. (2001) Axon–glia interactions and the domain organization of myelinated axons requires neurexin IV/Caspr/Paranodin. *Neuron*, **30**, 369–383.

Boyle,M.E., Berglund,E.O., Murai,K.K., Weber,L., Peles,E. and Ranscht,B. (2001) Contactin orchestrates assembly of the septate-like junctions at the paranode in myelinated peripheral nerve. *Neuron*, **30**, 385–397.

Coetzee,T., Fujita,N., Dupree,J., Shi,R., Blight,A., Suzuki,K., Suzuki,K., Popko,B. (1996) Myelination in the absence of galactocerebroside and sulfatide: normal structure with abnormal function and regional instability. *Cell*, **86**, 209–219.

Dupree,J.L., Girault,J.A. and Popko,B. (1999) Axo-glial interactions regulate the localization of axonal paranodal proteins. *J. Cell Biol.*, **147**, 1145–1152.

Faivre-Sarrailh,C., Gauthier,F., Denisenko-Nehrbass,N., Le Bivic,A., Rougon,G. and Girault,J A. (2000) The glycosylphosphatidyl inositol-anchored adhesion molecule F3/contactin is required for surface transport of paranodin/contactin-associated protein (caspr). *J. Cell Biol.*, **149**, 491–502.

Fournier,A.E., GrandPre,T. and Strittmatter,S.M. (2001) Identification of a receptor mediating Nogo-66 inhibition of axonal regeneration. *Nature*, **409**, 341–346.

Gennarini,G., Durbec,P., Boned,A., Rougon,G. and Goridis,C. (1991) Transfected F3/F11 neuronal cell surface protein mediates intercellular adhesion and promotes neurite outgrowth. *Neuron*, **6**, 595–606.

Girault,J.A. and Peles,E. (2002) Development of nodes of Ranvier. *Curr. Opin. Neurobiol.*, **12**, 476–485.

Hu,W.H., Hausmann,O.N, Yan,M.S., Walters,W.M., Wong,P.K. and Bethea,J.R. (2002) Identification and characterization of a novel Nogo-interacting mitochondrial protein (NIMP). *J. Neurochem.*, **81**, 36–45.

Huber,A.B., Weinmann,O., Brosamle,C., Oertle,T. and Schwab,M.E. (2002) Pattern of Nogo mRNA and protein expression in the developing and adult rat and after CNS lesions. *J. Neurosci.*, **22**, 3553–3567.

Ishibashi,T. *et al*. (2002) A myelin galactolipid, sulfatide, is essential for maintenance of ion channels on myelinated axon but not essential for initial cluster formation. *J. Neurosci.*, **22**, 6507–6514.

Kazarinova-Noyes,K. *et al*. (2001) Contactin associates with Na^+ channels and increases their functional expression. *J. Neurosci.*, **21**, 7517–7525.

Lee,S., Takeda,Y., Kawano,H., Hosoya,H., Nomoto,M., Fujimoto,D., Takahashi,N. and Watanabe,K. (2000) Expression and regulation of a gene encoding neural recognition molecule NB-3 of the contactin/F3 subgroup in mouse brain. *Gene*, **245**, 253–266.

Lei,G. *et al*. (2002) Gain control of N-methyl-D-aspartate receptor activity by receptor-like protein tyrosine phosphatase α. *EMBO J.*, **21**, 2977–2989.

Liu,H., Ng,C.E. and Tang,B.L. (2002) Nogo-A expression in mouse central nervous system neurons. *Neurosci. Lett.*, **328**, 257–260.

McGee,A.W., Strittmatter,S.M. (2003) The Nogo-66 receptor: focusing myelin inhibition of axon regeneration. *Trends Neurosci.*, **26**, 193–198.

Nakahira,K., Shi,G., Rhodes,K.J., Trimmer,J.S. (1996) Selective interaction of voltage-gated K^+ channel β-subunits with α-subunits. *J. Biol. Chem.*, **271**, 7084–7089.

Peles,E., Joho,K., Plowman,G.D. and Schlessinger,J. (1997) Close similarity between *Drosophila* neurexin IV and mammalian Caspr protein suggests a conserved mechanism for cellular interactions. *Cell*, **88**, 745–746.

Poliak,S., Gollan,L., Martinez,R., Custer,A., Einheber,S., Salzer,J.L., Trimmer,J.S., Shrager,P. and Peles,E. (1999) Caspr2, a new member of the neurexin superfamily, is localized at the juxtaparanodes of myelinated axons and associates with K^+ channels. *Neuron*, **24**, 1037–1047.

Poliak,S., Gollan,L., Salomon,D., Berglund,E.O., Ohara,R., Ranscht,B. and Peles,E. (2001) Localization of Caspr2 in myelinated nerves depends on axon–glia interactions and the generation of barriers along the axon. *J. Neurosci.*, **21**, 7568–7575.

Popko,B. (2000) Myelin galactolipids: mediators of axon–glial interactions? *Glia*, **29**, 149–153.

Rasband,M.N. and Trimmer,J.S. (2001) Developmental clustering of ion channels at and near the node of Ranvier. *Dev. Biol.*, **236**, 5–16.

Rasband,M.N., Trimmer,J.S., Schwarz,T.L., Levinson,S.R., Ellisman, M.H., Schachner,M. and Shrager,P. (1998) Potassium channel distribution, clustering and function in remyelinating rat axons. *J. Neurosci.*, **18**, 36–47.

Rasband,M.N., Trimmer,J.S., Peles,E., Levinson,S.R. and Shrager,P. (1999) K^+ channel distribution and clustering in developing and hypomyelinated axons of the optic nerve. *J. Neurocytol.*, **28**, 319–331.

Scherer,S.S. and Arroyo,E.J. (2002) Recent progress on the molecular organization of myelinated axons. *J. Peripher. Nerv. Syst.*, **7**, 1–12.

Shimazaki,K., Hosoya,H., Takeda,Y., Kobayashi,S. and Watanabe,K. (1998) Age-related decline of F3–contactin in rat hippocampus. *Neurosci. Lett.*, **245**, 117–120.

Spiegel,I., Salomon,D., Erne,B., Schaeren-Wiemers,N. and Peles,E. (2002) Caspr3 and caspr4, two novel members of the caspr family are expressed in the nervous system and interact with PDZ domains. *Mol. Cell. Neurosci.*, **20**, 283–297.

Swanborg,R.H. (2001) Experimental autoimmune encephalomyelitis in the rat: lessons in T-cell immunology and autoreactivity. *Immunol. Rev.*, **184**, 129–135.

Taketomi,M., Kinoshita,N., Kimura,K., Kitada,M., Noda,T., Asou,H., Nakamura,T. and Ide,C. (2002) Nogo-A expression in mature oligodendrocytes of rat spinal cord in association with specific molecules. *Neurosci. Lett.*, **332**, 37–40.

Trimmer,J.S. (1991) Immunological identification and characterization of a delayed rectifier K+ channel polypeptide in rat brain. *Proc. Natl Acad. Sci. USA*, **88**, 10764–10768.

Vabnick,I. and Shrager,P. (1998) Ion channel redistribution and function during development of the myelinated axon. *J Neurobiol.*, **37**, 80–96.

Vabnick,I., Trimmer,J.S., Schwarz,T.L., Levinson,S.R., Risal,D. and Shrager,P. (1999) Dynamic potassium channel distributions during

axonal development prevent aberrant firing patterns. *J. Neurosci.*, **19**, 747–758.

Wang,X., Chun,S.J., Treloar,H., Vartanian,T., Greer,C.A. and Strittmatter,S.M. (2002) Localization of Nogo-A and Nogo-66 receptor proteins at sites of axon-myelin and synaptic contact. *J. Neurosci.*, **22**, 5505–5515.

Woolf,C.J. (2003) No Nogo: now where to go? *Neuron*, **38**, 153–156.

Xiao,Z.C., Taylor,J., Montag,D., Rougon,G. and Schachner,M. (1996) Distinct effects of tenascin-R domains in neuronal cell functions and identification of the domain interacting with the neuronal recognition molecule F3/F11. *Eur. J. Neurosci.*, **8**, 766–782.

Received January 28, 2003; revised September 8, 2003; accepted September 16, 2003